Environmental controls on zooplankton composition and distribution in Muchalat Inlet, Nootka Sound, B.C., Canada

McWhirter, Andrew C.[1]

School of Oceanography Senior Thesis
2015

[1] School of Oceanography, University of Washington, Seattle, WA 98105

Andrew C. McWhirter
School of Oceanography
University of Washington
1503 NE Boat Street
Seattle, WA 98105
drew808@uw.edu

keywords: zooplankton, composition, abundance, spatial distribution, PCA

ABSTRACT

This study investigates environmental controls on zooplankton populations within the estuarine Muchalat Inlet fjord basin in Nootka Sound, B.C., Canada. Five stations were sampled along an ecological gradient from exposed Nootka Sound towards the head of Muchalat Inlet. At each station, four samples were collected at different depth ranges of the upper 100 meters to distinguish vertical distribution of zooplankton, and environmental conditions were measured by CTD casts. Abundances of nine zooplankton groups were identified, including euphausiids, hyperiids, gammarids, chaetognaths, larvaceans, ostracods, *Oithona*, other small copepods, and large copepods. Principal component analysis was used to identify correlation of sample composition and environmental conditions. Vertical distributions of zooplankton groups were strongly associated with salinity and dissolved oxygen limitations, while horizontal distributions were likely controlled by water mass transport. This study assists future conservation efforts and ecological modeling of dynamic estuarine systems.

INTRODUCTION

Zooplankton populations are vitally important in marine food webs and significantly influence marine biogeochemical cycles throughout the world's oceans. All species are heterotrophic or omnivorous, feeding on photosynthetic algae, bacteria, or smaller zooplankton, and function as primary consumers of autotrophic organisms (Gentleman et al. 2003). Zooplankton commonly serve as the primary food source for higher trophic levels, and their distributions often limit higher and

lower trophic level populations (Frederiksen et al. 2006). In addition, zooplankton strongly influence the global carbon cycle and the transfer of carbon between the atmosphere and the ocean. Past work from Longhurst (1991) and Shaffer (1993) expresses this concept in terms of a 'biological pump'. Phytoplankton use energy from the sun to convert inorganic carbon and other essential nutrients into organic matter. This organic matter is then consumed by primary consumers (zooplankton); most of which is recycled within the system. However, some of this organic material is exported downwards from the surface mixed layer to the deep ocean via diel vertical migration of zooplankton, and enhanced by accelerated sinking of dense fecal matter and marine snow aggregations (Turner 2002). Carbon export to the deep ocean advances diffusion of inorganic carbon into the surface mixed layer, linking atmosphere CO_2 and ocean dissolved inorganic carbon (DIC) concentrations, thus influencing the global carbon cycle. Identifying the environmental parameters that control zooplankton composition, abundance and distribution is essential to develop a better understanding of the food web dynamics of specific marine systems, with broader implications for global biogeochemical cycles.

Relatively little is known about zooplankton community composition, abundance, distribution, and population dynamics in Nootka Sound (Pelle 2015). This estuarine fjord basin is located on the west coast of Vancouver Island, and includes Muchalat Inlet and Tahsis Inlet, which are both long and narrow embayments with substantial river input gated by sills near the mouth. These inlets are distinct from fjord systems of the mainland coast and are generally shorter and shallower, with shallower sills. Maximum freshwater input from river runoff occurs

in the winter, in contrast to mainland inlets (Pickard 1963). Muchalat Inlet is wider and deeper than Tahsis Inlet, and has significantly more freshwater input from the Burman River, Gold River, and Houston River. Pelle's (2015) study on zooplankton species composition and depth-based habitat preference in Nootka Sound found that zooplankton composition, abundance, and distribution varied substantially between distinct regions of this basin; Muchalat Inlet, Tahsis Inlet, and Nootka Sound. Total abundance and biomass of zooplankton samples from Muchalat Inlet were found to be much lower compared to that of Tahsis Inlet and exposed Nootka Sound (Pelle 2015). This study focuses on identifying the key environmental parameters that exert control over zooplankton composition, abundance, and distribution within Muchalat Inlet.

Muchalat Inlet receives freshwater discharge from the Burman River, Gold River, and Houston River, as well as numerous creeks surrounding the basin. The Gold River is the largest of the three, reaching average maximum discharge of 150-200 m^3/s from mid October through January, according to the Government of Canada Wateroffice record (1956-2014). The inlet is gated by the Williamson Sill, which acts as a barrier restricting the free interchange of nutrient rich oceanic water and deep basin water of Muchalat Inlet (Gorsky et al. 2000a, Pickard 1963). Stratification in estuarine systems typically results from general two-layer vertical circulation, with subsurface inflow of denser, saline oceanic water and surface outflow of less dense, lower salinity water (Laprise and Dodson 1994, Silva and Vargas 2014).

Ecologically limiting factors including salinity, dissolved oxygen, chlorophyll, pH, and temperature vary substantially due to stratification effects. Dissolved oxygen concentrations within estuarine systems are controlled by oceanic supply, freshwater input, atmospheric diffusion, biological productivity, and respiration. Stratification combined with particulate organic matter respiration can create a steep dissolved oxygen gradient between surface and subsurface layers, significantly limiting the habitable range of aerobic organisms. Oxygen thresholds relevant to zooplankton are usually defined as oxic (8.0-2.0 ml/l O_2), dysoxic (2.0-0.2 ml/l O_2), suboxic (0.2-0.0 ml/l O2), and anoxic (0.0 ml/l O_2), with concentrations between oxic and anoxic regarded as hypoxic conditions (Tyson and Pearson 1991). Characteristic vertical profiles of Muchalat Inlet in May (1959) and June (1960) from Pickard (1963) showed salinity increasing with depth to approximately 100m, dissolved oxygen decreasing with depth reaching anoxic conditions below 200m, and temperature decreasing with depth.

Considering the environmental variability of estuarine systems, the effects are expected to be prevalent on zooplankton population composition, abundance and distribution in Muchalat Inlet. It is hypothesized that total zooplankton abundance and species composition will be greatest in oceanic Nootka Sound and nearer the mouth of Muchalat Inlet, where there is more exchange of nutrient-rich seawater. Lower zooplankton abundance and diversity is predicted towards the head of Muchalat Inlet, where salinity and dissolved oxygen are projected to be lower due to considerable river discharge. Dissolved oxygen concentration is predicted to limit distributions above hypoxic and anoxic layers, and greater

concentrations are expected nearer the surface where dissolved oxygen is maximum (Pickard 1963).

Pelle's (2015) study found *Oithona* to be the most abundant zooplankton in Muchalat Inlet and throughout Nootka Sound. Oithonids are small Cycopoid copepods, usually 0.5-1mm in length, thought to be the most abundant zooplankton species throughout the world's oceans. *Oithona* are tolerant of a wide range of environmental conditions (Turner 2004). Therefore, *Oithona* are predicted to be the most abundant organism across all samples. Copepods are predicted to be the dominant zooplankton group observed, based on counts from Pelle (2015). Total zooplankton abundance is predicted to be greatest nearer the surface at night due to diel vertical migration (DVM) patterns common of larger species, and the opposite is predicted during the day (Hays 2003). Macrozooplankton groups are known to tolerate a narrower range of ecological conditions (Laprise and Dodson 1994). Thus, their distributions are predicted to be limited to regions exposed to significant oceanic influence.

This study examines environmental conditions limiting zooplankton populations within estuarine Muchalat Inlet. Understanding the mechanisms controlling zooplankton populations, and the associated ecological implications of variable environmental conditions, is essential to improve ecological modeling and conservation of these dynamic and ecologically important coastal systems. Previous zooplankton population studies used full water column vertical net tows to collect zooplankton samples and identify spatial distribution within an investigatory basin (Laprise and Dodson 1994, Stalder and Marcus 1997, Turner 2004, Pelle 2015).

This study additionally distinguishes vertical distribution across all sampling stations to identify variation among zooplankton assemblages at different depths, and associated ecological conditions.

A secondary research goal of this study explored an alternative method of zooplankton population sampling by applying a technological approach. The objective was to design, build and deploy a low-cost underwater video profiler (UVP) prototype to assess the potential of this technique for future applications. Previous work done by Gorsky et al. has utilized a similar instrument to study zooplankton distribution in Norwegian Fjord systems (Gorsky et al. 2000a), as well as aggregate dynamics in the North Mediterranean (Gorsky et al. 2000b), demonstrating the versatility of this method. This approach offers distinct advantages for future zooplankton population studies, providing a low-cost means to increase sample size, and can be utilized as a Eulerian or Lagrangian instrument documenting variability of zooplankton populations in both time and space. Detailed information on UVP sensor design, data collection, and preliminary results are provided in *Appendix VI*.

METHODS

Overview

Zooplankton samples were collected by vertical net tows at each station. Collecting samples in this way allows for precise identification and analysis of zooplankton composition. However, this method is limited by the volume of water sampled, the amount of time required to collect each individual sample, and the cost

of ship time needed to acquire samples at sea. We use this approach as the focus of this study to explore the variation in zooplankton composition, abundance and vertical distribution within estuarine Muchalat Inlet to that outside of Muchalat Inlet, from Nootka Sound more exposed to oceanic conditions. We also investigate variation among Muchalat Inlet stations sampled at night to one station sampled during daylight.

Vertical Net Tow Sampling

Zooplankton samples were collected from Nootka Sound and Muchalat Inlet aboard the R/V *Thomas G. Thompson* during the University of Washington School of Oceanography senior thesis cruise, December 10th-20th, 2015. Five sampling stations were selected prior to the cruise, including oceanic station C05 located outside of Muchalat Inlet in exposed Nootka Sound, and estuarine stations C08, C09, C10, and C11 spanning from the mouth to the head of Muchalat Inlet (Image 1). The upper 100 meters of the water column was sampled at each station by a series of vertical net tow deployments. Stations C05, C08, C09, and C10 were sampled at night, and station C11 was sampled during the day. CTD casts preceded zooplankton sampling at each station to generate vertical profiles of salinity, dissolved oxygen, fluorescence, pH, and temperature.

Image 1. Station map of Nootka Sound focusing in on Muchalat Inlet.

Zooplankton samples were obtained using a 0.5m diameter, 211µm mesh closing net, which allowed samples to be collected at different depth ranges within the upper 100 meters of the water column. A series of four vertical net tows were carried out at each station to collect samples from 100-75m, 75-50m, 50-25m, and 25-0m depth ranges, in sequential order. The closing net apparatus was triggered at the upper depth limit of a given sample by sending a 5kg messenger down the winch cable to activate the release mechanism. The zooplankton net was thoroughly rinsed using a saltwater hose once the net was raised out of the water to ensure that all of the organisms captured in the net were washed into the codend. The net was then carefully lowered onto the deck, securing the codend and all of the contained organisms. The codend was carefully removed and the contents were transferred into 750mL jars. Each sample was fixed in a 5% formalin solution and preserved for later laboratory analysis.

Laboratory Procedures

Organisms contained within each sample were quantified using laboratory procedures provided by Kathy Newell and Julie Keister. Samples were filtered into a 200μm mesh sieve and separated from the seawater-formalin (5%) solution. Organisms were transferred into a graduated cylinder and diluted with freshwater to a fixed volume of 300ml, then transferred back into a 750ml jar. Three aliquots were isolated from the total 300ml sample using a 5ml Stempel pipette, and transferred into a zooplankton counting tray. The contents of each aliquot were counted under a 15x magnification dissecting scope using a handheld tally counter. Zooplankton groups identified included euphausiids, hyperiids, gammarids, larvaceans, chaetognaths, ostracods, *Oithona*, other small copepods (<2mm), and large copepods (>2mm). Abundances were standardized to $1m^3$ by multiplying the sum of aliquot counts by the dilution factor of 20 (300ml/15ml), and dividing by the volume of water sampled ($\pi*0.5m^2$ x 25m). Samples were classified by station and max depth of sample, in the notation 'station_depth'.

RESULTS

Zooplankton Composition & Distribution

Zooplankton composition varied considerably with regard to spatial distribution, both vertically and across sampling stations. Abundances and proportion of zooplankton groups (m^{-3}) identified in each sample are reported in *Appendix I* (Table 1, Table 2). The greatest overall zooplankton abundance was observed at station C05 (Figure 3). Concentration increased with depth at this

station (Figure 1). Copepods were the most abundant zooplankton group in all samples except C09_75. Maximum total zooplankton concentration of 3573/m^3 was observed in sample C05_100, where copepods accounted for 97.2% of organisms. Minimum total zooplankton concentration of 103/m^3 was observed in sample C09_75, where copepods accounted for 31.6% of organisms. Among Muchalat Inlet stations, total zooplankton abundance was greatest near the mouth (C08) and head (C11) of Muchalat Inlet, and lowest in the middle of the estuary (C09) (Figure 3). The greatest total zooplankton abundance was observed at station C11, sampled in daylight. All Muchalat stations showed little variability in total zooplankton abundance among 25m and 50m samples (Figure 1). Stations C08, C09, and C10 sampled at night showed minimum total zooplankton abundance in 75m samples. However, station C11 sampled during the day showed total zooplankton abundance decreasing with depth, and concentration in the 75m sample was much greater than that of Muchalat stations sampled at night.

The greatest concentrations and proportions of euphausiids, hyperiids, and gammarids were found in C05_75, followed by C10_75. Proportions of these macrozooplankton species were very similar in both C05_75 and C10_75 samples (Figure 2, Table 2), though concentrations were much greater in C05_75 (Figure 1, Table 1). Euphausiids and hyperiids were found in the deeper samples from these two stations (C05_100 and C10_100), but were not observed in 100m samples from other stations. Gammarids were identified in 50m and 75m samples from C05, C08, and C10, as well as 25m and 75m samples from C09 (Table 1). There were no macrozooplankton crustaceans found in C11 samples.

The largest proportion of ostracods was found to be 63.2% in sample C09_75, where the proportion of total copepods is a minimum 31.6%. This observation was consistent with 75m samples from adjacent stations C08 and C10 (Table 2, Figure 2). The maximum proportion of ostracods across 25m samples was observed at C09. The proportion of ostracods in 100m samples increased from C05 to C11, towards the head of Muchalat Inlet (Figure 2). Abundance of ostracods was observed to increase with depth at all Muchalat Stations except station C09, where ostracod concentration was greater in the 25m sample than the 50m sample (Table 1).

Copepod populations, representing the majority of zooplankton collected, differed substantially across stations and depths. Station C05 outside of Muchalat Inlet had relatively low copepod density of 657/m^3 in the upper 50 meters (C05_25 and C05_50), density doubled in the 75m sample, and increased to a maximum copepod density of 3471/m^3 in the 100m sample. The proportion of *Oithona* remained relatively constant with depth, while the proportion of other small copepods decreased with depth, and the proportion of large copepods increased with depth. (Figures 1 & 2, Tables 1 & 2)

Within Muchalat Inlet, station C08 showed maximum copepod density of 1381/m^3 in the 25m sample, and minimum copepod density of 139/m^3 in the 75m sample, where 50m and 100m samples had similar densities of 962/m^3 and 941/m^3 respectively. *Oithona* represented over half of the copepod population in the upper 50m and increased from 51% in C08_25 to 63% in C08_50, but declined sharply down to 0% in C08_75, then increased to 58% of total copepod abundance in C08_100. The proportion of other small copepods was more consistent with depth,

decreasing from 36% in C08_25 to 24% in C08_50, slightly increased to 29% in C08_75, then decreased to 17% in C08_100. The proportion of large copepods was a minimum 13% in C08_25 and C08_50, then increased significantly to 70% in C08_75, and decreased to 26% of total copepod abundance in C08_100. (Figures 1 & 2, Tables 1 & 2)

A similar pattern was seen at station C09, where total copepod densities increase from 473/m^3 in 25m the sample to 611/m^3 in the 50m sample, but decreased sharply down to 103/m^3 in the 75m sample, and then increased to maximum copepod density of 843/m^3 in the 100m sample. The proportion of *Oithona* decreased from 51% in C09_25 to 37% in C09_50, and was 0% in C09_75, but increased drastically to 76% in C09_100. The proportion of other small copepods increased with depth in the upper 75 meters, from 30% in C09_25 to 44% in C09_50 to 63% in C09_75, but decreased sharply to 14% in C09_100. The proportion of large copepods remained constant at 19% in 25m and 50m samples, then increased to 38% in C09_75, but decreased sharply to 10% in C09_100. (Figures 1 & 2, Tables 1 & 2)

Station C10 had maximum copepod abundance of 1218/m^3 in the 25m sample, reduced to 839/m^3 in the 50 m sample, then deceased sharply to 187/m^3 in the 75m sample, and increased slightly to 314/m^3 in the 100m sample. The proportion of *Oithona* increased from 25% in C10_25 to 59% in C10_50, but decreased sharply to 7% in C10_75, then increased to 48% in C10_100. The proportion of other small copepods decreased from 74% in C10_25 to 34% in C10_50, then increased to 50% in C10_75, and decreased down to 40% in C10_100.

The proportion of large copepods increased from 1% in C10_25 to 7% in C10_50, then increased considerably to 44% in C10_75, but was reduced to 12% of total copepod abundance in C10_100. (Figures 1 & 2, Tables 1 & 2)

For station C11 sampled in daylight, total copepod abundance increased slightly from 1442/m^3 in the 25m sample to 1524/m^3 in the 50m sample, then decreased to 1092/m^3 in the 75m sample, and decreased sharply to 183/m^3 in the 100m sample. The proportion of *Oithona* increased from 34% in C11_25 to 83% in C11_50, decreased to 53% in C11_75, and further down to 20% in C11_100. The proportion of other small copepods decreased from 64% in C11_25 to 17% in C11_50, increased to 45% in C11_75, and further up to 53% in C11_100. The proportion of large copepods was 0% in the upper 50m sampled, increased slightly to 2% in C11_75, and increased considerably to 27% in C11_100. (Figures 1 & 2, Tables 1 & 2)

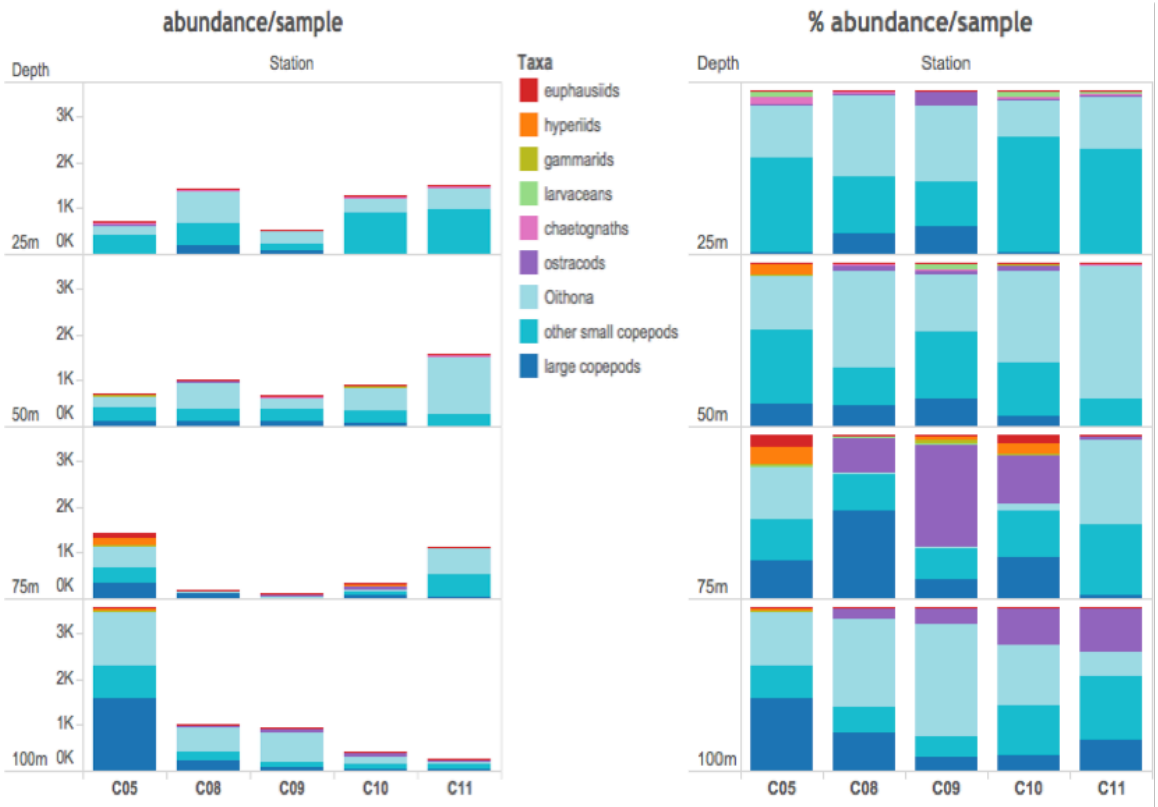

Figure 1. Sum of zooplankton abundance/(m^3) for each sample, ranging from 0 to 1,573. Color shows details about Taxa.

Figure 2. Percent of total abundance/(m^3) for each sample. Color shows details about Taxa.

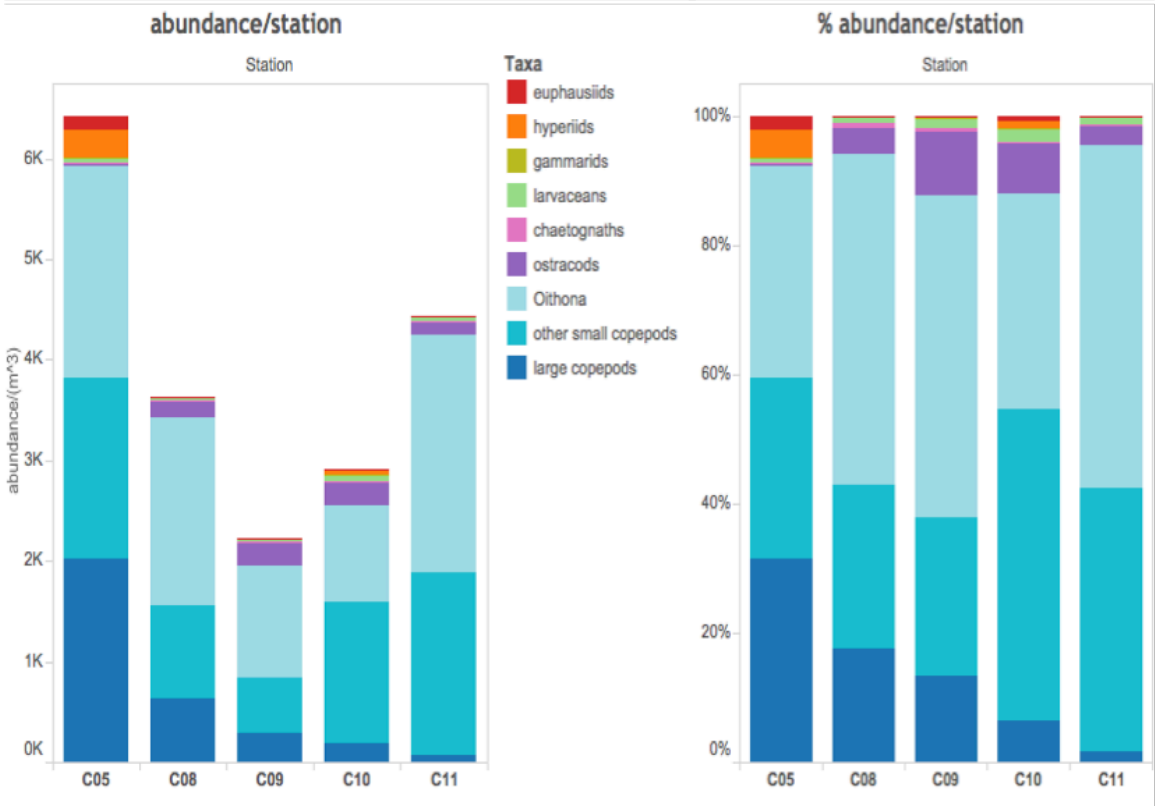

Figure 3. Sum of zooplankton abundance/(m^3) for each Station. Color shows details about Taxa.

Figure 4. Percent of total abundance/(m^3) for each Station. Color shows details about Taxa.

Environmental Conditions

The environmental parameters that characterize the water column conditions at each station are reported in *Appendix II* (Table 3). The shallowest stations were found outside of Muchalat Inlet at C05 (169m) and near the head of Muchalat Inlet at C11 (159m). Station depth was 273m at C08, and maximum station depth was observed in the middle of Muchalat Inlet at stations C09 (362m) and C10 (360m). Environmental parameters are presented as mean values of associated sample depth ranges (100-75m, 75-50m, 50-25m, 25-0m). Salinity increased with depth across all stations. Mean salinity of the upper 25 meters decreased from station C05 towards the head of Muchalat Inlet at station C11, where minimum salinity of 29.9_{PSU} was observed. Maximum salinity was observed at station C05 corresponding to C05_100 (32.9_{PSU}), and decreased from the mouth to the head of Muchalat Inlet across 100m samples. An inverse trend was observed in dissolved oxygen concentrations, with values decreasing with depth across all stations. Mean dissolved oxygen concentrations of the upper 25 meters were greater across Muchalat stations compared to station C05 outside of Muchalat Inlet. Minimum mean dissolved oxygen concentrations were associated with 100m samples from stations C05 ($0.15_{ml/l}$) and C11 ($0.12_{ml/l}$), and reached suboxic conditions ($<0.2_{ml/l}$). Maximum dissolved oxygen concentration associated with the 25m sample from station C08. Maximum dissolved oxygen concentrations for mid-depth samples (75m and 50m) were observed at station C05. Mean dissolved oxygen values associated with 50m and 75m samples are relatively consistent across Muchalat stations. Mean pH values decreased with depth across Muchalat

stations. However, at station C05, mean pH increased from 25m to 50m, then decreased from 50m to 100m. Maximum pH associated with 25m samples from stations C10 and C11, and the lowest pH across 25m samples associated with station C05. Minimum pH across all samples associated with C05_100 and C08_100. Temperature profiles were similar across all stations, though a mid-water maximum was associated with 50m samples at Muchalat stations, reaching maximum mean temperature at C11_50. Fluorescence values were greatest outside of Muchalat Inlet at station C05, and maximum fluorescence associated with C05_50. Profiles showed decreased fluorescence with depth for Muchalat stations, and values were relatively consistent across stations C08, C09, and C10, where station C11 had slightly greater fluorescence.

Principal Component Analysis

Principal component analysis (PCA) was used to determine which zooplankton groups explain the greatest variance in sample composition (*Appendix III and IV)*. This statistical method takes the mean composition across all samples and sets that as the origin of a three-dimensional coordinate system. Each zooplankton taxa defines a distinct dimension in space, and the variation attributed to each group is represented as a vector from the origin. Each observation, or sample, is then plotted in three-dimensional space relative to deviation from mean sample composition. Two orthogonal planes that explain the greatest variation in the three-dimensional distribution of sample composition are defined as Principal Component 1 (PC1) and Principal Component 2 (PC2). A biplot can then be

generated from PC1 and PC2, where the principal components are expressed as the x and y axes of an ordination plot. Variation from mean sample composition is displayed in a two-dimensional coordinate plane to show the distribution of samples corresponding to PC1 and PC2. The eigenvectors displayed in the PCA plots represent each zooplankton group and distinguish variation explained by PC1 and PC2. Environmental parameters were added to PCA plots by scaling circle points to the mean value of each parameter, corresponding to the associated depth range for each sample. The distribution of samples and corresponding parameters displayed on PCA plots enables recognition of correlation between sample composition and environmental conditions.

The first PCA, denoted 'PCA-all', included all samples and is presented in *Appendix III*, with associated environmental parameters. Principal component 1 ($PC1_a$) explained 37% of variation in sample composition, and was positively correlated with concentrations of macrozooplankton groups (euphausiids, hyperiids, and gammarids). Principal component 2 ($PC2_a$) explained an additional 29% of variation in sample composition, and was most positively correlated with concentrations of other small copepods and chaetognaths, and negatively correlated with concentration of ostracods. 'PCA-all' showed samples C05_75, and C05_100 had the greatest variation in sample composition, positively correlated with $PC1_a$. Variation in sample composition for all other samples was highly correlated with $PC2_a$, and thus showed significant distribution along this axis, with minimal variation along $PC1_a$. Zooplankton samples from station C05 outside of Muchalat Inlet were responsible for the majority of the variation in mean sample composition

identified by this principal component analysis that included all samples (*Appendix III*).

A second PCA ('PCA-Muchalat') was generated that excludes oceanic C05 samples to identify variation in species composition among estuarine Muchalat Inlet samples. 'PCA-Muchalat' plots are presented in *Appendix IV*, with corresponding environmental parameters. Samples were much more evenly distributed in 'PCA-Muchalat', compared to 'PCA-all', and clustered samples with similar zooplankton composition are identified. Principal component 1 ($PC1_m$) explained 41% of variation in sample composition, and was most positively correlated with concentration of ostracods, and most negatively correlated with concentration of chaetognaths. Principal component 2 ($PC2_m$) explained an additional 21% of variation in sample composition, and was most positively correlated with concentration of other small copepods, and most negatively correlated with concentration of large copepods. Samples C08_75, C09_25, C10_100 and C11_100 were positively correlated with $PC1_m$, slightly negatively correlated with $PC2_m$, and tightly clustered along the 'ostracod' axis. These samples had similar zooplankton compositions and relatively low concentrations. Variation was highly correlated to concentration of ostracods, and inversely correlated to concentrations of other small copepods and chaetognaths (Figure 1, Figure 2). Samples C08_100 and C09_100 were negatively correlated with $PC2_m$, and paired along the 'large copepod' axis. Total abundance, composition, and proportions were very similar in these samples, where C09_100 had slightly lower zooplankton density and fewer large copepods (Figure 1, Figure 2). Samples C08_25, C09_50, C11_50, and C11_75 were

loosely grouped and negatively correlated with $PC1_m$. Variation in these samples was associated with concentrations of *Oithona*, other small copepods, and chaetognaths (Figure 1, Figure 2). Samples C10_25 and C11_25 were negatively correlated with $PC1_m$, positively correlated with $PC2_m$, and isolated along the 'chaetognath' and 'other small copepods' axis. Variation from mean composition was associated with concentrations of these two zooplankton groups, where sample C11_25 had greater abundance of *Oithona* (Figure 1, Figure 2). Samples C09_75, C10_50 and C10_75 were positively correlated with $PC1_m$ and $PC2_m$, associated with concentrations of macrozooplankton and ostracods. Of these samples, C09_75 was least correlated to $PC2_m$. Sample C10_75 showed the greatest deviation from the mean across all Muchalat samples, corresponding to maximum macrozooplankton concentrations (Figure 1, Figure 2).

Environmental parameter values plotted on 'PCA-Muchalat' identify the conditions associated with sample composition, based on sample distribution and grouping in the biplot. Samples grouped along the 'ostracod' axis correlated with high salinity, low dissolved oxygen, low pH (except C09_25), and low temperature conditions. Similarly, samples grouped along the 'large copepod' axis correlated with high salinity, low dissolved oxygen, low pH and low temperature conditions. Samples negatively correlated with $PC1_m$ and minimally correlated with $PC2_m$ showed variation of high and low salinity values, median dissolved oxygen, higher pH, and variation of medium and high temperature conditions. Samples highly correlated with 'chaetognaths' and 'other small copepods' associated with minimum salinity, maximum dissolved oxygen, maximum pH, and median temperature

conditions. Samples distributed along the macrozooplankton axes associated with medium-high salinity, lower dissolved oxygen, medium pH, and medium temperature conditions relative to other samples. The sample that was closest to mean composition from Muchalat stations was C08_50, and associated with median values for all parameters investigated. Zooplankton composition did not correlate significantly with depth. (*Appendix III, IV).*

Shannon Wiener Diversity Index

Zooplankton diversity varied substantially among samples, and results from Shannon Wiener Diversity Index are reported in *Appendix V*. There was no significant relationship observed in sample diversity, both horizontally across stations and vertically with depth. Maximum diversity index values were associated 75m samples from stations C10 and C05. Sample C05_75 had much greater zooplankton abundance, but C10_75 had the greatest overall diversity. Minimum diversity was observed in sample C11_50. The greatest diversity in 100m samples was found at stations C10 and C11, where zooplankton abundance is minimal.

DISCUSSION

Significant variation in zooplankton composition identified among samples from exposed Nootka Sound (station C05) and estuarine Muchalat Inlet (stations C08, C09, C10 and C11) supports the hypothesis that zooplankton composition and abundance is greater in regions exposed to more oceanic exchange and reduced stratification. However, the vertical distribution of zooplankton and environmental

conditions observed at this station were inconsistent with hypothesized optimal conditions predicted to be associated with maximum zooplankton density. Zooplankton concentration was predicted to be greatest near the surface at night based on diel vertical migration patterns, and maximum dissolved oxygen concentrations (Pickard 1963, Hays 2003). Observed concentrations generally increased with depth and maximum zooplankton abundance was found in sample C05_100, corresponding to suboxic conditions. The 50m and 25m samples from station C05 had much lower zooplankton concentrations than deeper samples. Copepod abundance was significantly lower in these upper 50m samples, especially large copepods, expected to be in greatest concentrations near the surface at night (Hays 2003). The environmental conditions measured at Nootka station C05 did not show any major anomalies compared to Muchalat stations that could explain lower densities observed in the 25m and 50m samples, and much greater densities observed in 75m and 100m samples. In fact, maximum mean dissolved oxygen values across all samples were observed in the upper 50m at station C05. Therefore, samples from this depth range were predicted to have the highest concentration and species composition. These 25m and 50m samples from oceanic C05 were highly correlated to Muchalat samples in a Principal Component Analysis of zooplankton composition at all stations (*Appendix III - 'PCA-all'*). This suggests that physical mechanisms may have greater influence on zooplankton composition and abundance at this station than the parameters investigated. A proposed hypothesis that would explain this observation is that surface outflow from Muchalat Inlet transports small copepods from the estuary where large copepod concentrations

are low, and overall zooplankton abundance is much lower compared to deeper oceanic C05 assemblages. A similar process may be delivering high concentrations of zooplankton in deeper water of oceanic origin, which would explain maximum zooplankton densities and associated conditions observed for C05_75 and C05_100 samples (Laprise and Dodson 1994).

Across Muchalat stations, C11 at the head of the Inlet and sampled in daylight had the greatest total zooplankton abundance, which was largely unpredicted. Here, stratification was maximum, and all environmental parameters showed the greatest variation with depth across all stations, seen in *Appendix II.* Zooplankton concentration decreased with depth at station C11, where stations sampled at night showed the opposite or an irregular trend. The 25m sample contained maximum concentration of other small copepods observed across all samples, and the 50m sample contained maximum concentration of *Oithona* observed across all samples. The variation and distribution patterns observed are likely influenced by a variety of factors. The inverse relationship of *Oithona* and other small copepod abundance may be driven by biotic interactions such as competition for resources, where one group has an ecological advantage over the other at different depth ranges and associated conditions. Minimal abundances of large copepods were found in samples C11_75 and C11_100, and may be displaced species from oceanic origin transported up-inlet in the oceanic deep layer created by estuary circulation, and are likely vertically constrained by lower salinities in the upper water column and suboxic and anoxic conditions below (Laprise and Dodson 1994). Zooplankton species found in samples from the head of Muchalat Inlet are likely representative of

a persistent population comprising euryhaline species adapted to true estuarine conditions of lower salinity and significant stratification, and capable of recruiting new generations (Laprise and Dodson 1994). The observed vertical distribution may best be explained by these smaller copepod species having reduced predatory avoidance behaviors or less need for such behavior, and thus might not participate in diel vertical migration demonstrated by larger copepod species. Another possible explanation may be that these smaller copepod species exhibit reverse migration behaviors, and migrate to the surface as predator species migrate downward during the day. These euryhaline species may also be adapted to estuarine conditions while their predators are not tolerant, and therefore they concentrate in the upper water column beyond the habitable limits of larger zooplankton predators.

Minimum total zooplankton abundance observed at station C09, followed by total abundances of adjacent stations C10 and C08, might also be a result of horizontal advection currents characteristic of estuary circulation (Figures 1 and 3) (Laprise and Dodson 1994). Inflow of dense oceanic water may carry associated zooplankton species up the estuary away from their population center, where limited ecological tolerance of estuarine conditions prevents recruitment and may cause mortality. The same is predicted for euryhaline and estuarine adapted species habiting the less dense upper layer, and transported towards the mouth of the estuary in surface outflow, away from their population centers at the head of the estuary. Therefore, the middle of the estuary is where both populations intermix, but are poorly adapted to diverging ecological conditions, thus recruitment and persistence are constrained, and zooplankton concentrations are reduced (Laprise

and Dodson 1994). Evidence supporting this hypothesis is shown in Figure 1, where greater zooplankton abundances are observed in 25m and 50m samples from stations C08, C09, and C10, representing euryhaline compositions, minimum abundance is observed in 75m samples, and increased zooplankton abundance is observed in 100m samples, representing oceanic compositions. Another indication of this suggested mechanism is the Shannon Wiener Diversity Index values for each sample, reported in *Appendix V*. Maximum diversity in 25m and 50m samples were found at station C09, and maximum diversity in 75m samples was found at station C10, in the middle of Muchalat Inlet, and associated with low zooplankton abundances.

The distribution of macrozooplankton groups, including euphausiids, hyperiids and gammarids, were found to be particularly interesting. As predicted, highest concentrations were observed in deeper oceanic samples from station C05, implying that euphausiids are not tolerant of lower salinity conditions (Laprise and Dodson 1994). However hyperiids dominated macrozooplankton assemblages at lower salinities, suggesting they may be tolerant to a greater range of salinity conditions. Interestingly, euphausiids and hyperiids were both found in C10_75 and hyperiids were also found in C09_75, in the middle of Muchalat Inlet, where total zooplankton abundance was minimum. Their regional distribution may be primarily influenced by biotic factors at these sampling locations, where vertical distribution is likely limited by abiotic conditions of the upper water column. Gammarids were found to be the least abundant macrozooplankton compared to euphausiids and hyperiids. Biotic factors are predicted controls on this relationship, such as

competition for resources or greater net avoidance due to enhanced swimming capabilities. Abiotic factors are not likely to control gammarid abundance and distribution observed, given that gammarids and hyperiids were found in the same samples and associated environmental conditions. All macrozooplankton are likely underestimated due to swimming capabilities enhancing net avoidance, which might be the primary control on variation of these groups across samples (Clutter and Anraku 1979). This is especially relevant for daylight samples from C11, when avoidance ability is further increases by visual awareness.

Large copepod concentrations were associated with high salinity and low dissolved oxygen conditions in deeper samples. Their distribution from oceanic C05 up Muchalat Inlet to C11 was likely predominantly controlled by water mass transport. Common circulation characteristics of estuaries may explain this distribution. This proposed controlling mechanism is supported by past work on zooplankton distribution in estuaries, and is evident in the environmental parameter data reported in this study. Laprise and Dodson (1994) conducted a similar study on zooplankton spatial distribution and diversity controls in St. Lawrence Estuary, Quebec, Canada, and found that estuary circulation exhibits significant control on zooplankton composition and distribution in estuarine systems. Applying their findings to Muchalat Inlet suggests circulation proceeds with inflow of dense oceanic, high salinity, low dissolved oxygen water from outside Muchalat Inlet displaced towards the head of Muchalat Inlet at depth as less dense, lower salinity, high dissolved oxygen water flows out of the estuary in the upper water column. Though, vertical distribution of large copepods is likely limited by

environmental conditions, especially salinity, as shown in Figure 1 & 2, *Appendix III,* and identified by principal component analysis (*Appendix IV)*. It may be that majority of large copepods found in Muchalat Inlet samples originated in oceanic waters outside the estuary, and were transported up the estuary in the dense, deep, high salinity, low dissolved oxygen water mass. Therefore, large copepods may be less tolerant to estuarine conditions and lower salinities in upper layers of the water column, limiting diel vertical migration and persistence of these organisms. This mechanism may explain the reduced abundance of large copepods towards the head of Muchalat Inlet as stratification increases and estuarine conditions are maximized (Laprise and Dodson 1994). However, large copepods may have also been underestimated, attributing sufficient swimming capabilities (Clutter and Anraku 1979).

In contrast, euryhaline groups including *Oithona* and other small copepods capable of tolerating a vast range of salinity and dissolved oxygen conditions were found to dominate zooplankton concentration across all samples, omitting C09_75 where minimum zooplankton concentration was observed. Their distributions are likely controlled by biotic factors and recruitment capability. Biological interactions pertaining to competition of resources are likely controlling euryhaline species distributions, where some species may be better adapted to conditions associated with different samples. Other small copepods seem to be more abundant in surface samples, where *Oithona* were found to be more abundance in most samples below 25 meters. Similarly, abundance of *Oithona* and other small copepods was lower in samples with greater concentrations of macrozooplankton and large copepods,

suggesting that predator-prey interactions may be limiting small copepod populations at these locations.

Proportion of ostracods increased as concentrations of other zooplankton groups decreased at stations where stratification was highest, and in samples associated with high salinity and low dissolved oxygen. Ostracod abundance was greatest in samples with minimum zooplankton concentrations, most notable in 75m and 100m samples from stations C09 and C10. Both biotic and abiotic factors are predicted to control abundance of this zooplankton group. The proportion of ostracods increased as the proportion of copepod decreased across 100m samples from the mouth towards the head of Muchalat Inlet. The data suggests competition for resources with euryhaline small copepods may be driving distribution. Lower abundances are observed nearer the surface at most stations, and low salinity may be limiting vertical distribution. These organisms are shown to tolerate suboxic conditions in 100m, and may be better adapted the low oxygen environment, reducing predation and resource competition with less adapted species.

Chaetognaths and larvaceans were found only in very low densities, and showed an inverse relationship with macrozooplankton and large copepod abundance. Thus, their distributions may be predominantly influenced by biotic factors, oppose to abiotic parameters. Chaetognath concentration was highly correlated to other small copepods concentration, identified in the PCA plots, indicating a predator-prey relationship may be the driving mechanism of chaetognath distribution. However, their vertical distributions may be limited by

high salinity and lower pH, since they were primarily found in upper 50m of the water column.

CONCLUSION

This investigation identified salinity and dissolved oxygen to be the dominant environmental controls correlating to zooplankton population composition and distribution in the estuarine Muchalat Inlet fjord system. Sampling of the four distinct depth ranges in the upper 100 meters at 5 sampling stations along the ecological gradient provided valuable insight on both horizontal and vertical distributions of zooplankton populations in this estuarine system. Horizontal distributions from oceanic Nootka Sound to the head of Muchalat Inlet are predicted to be controlled by water mass transport of general two-layer circulation, where outflow of less dense, lower salinity more oxygen rich water in the upper water column is displaced by inflow of denser oceanic, saline water, with lower dissolved oxygen concentrations at depth. Environmental conditions and water column stratification highly correlated with vertical distributions of zooplankton groups. Salinity appeared to exhibit the greatest control on tolerable habitat limits for larger zooplankton groups, confining displaced populations in the deeper oceanic layer. Dissolved oxygen concentration likely limited distributions of less tolerant groups above suboxic and anoxic conditions. Evidence from this study can be used to further investigate trophic interactions and food web dynamics of this system. A follow up study should be conducted throughout the growth season to observe the

seasonal variability of this system and the implications on zooplankton assemblages, and may yield very different results.

Acknowledgements

I would like to thank the University of Washington School of Oceanography for this amazing opportunity to participate in a research cruise aboard the R/V *Thomas G. Thompson.* Many thanks to the R/V *Thomas G. Thompson* crew for all their help at sea ensuring a safe trip and assistance with data collection. Much appreciation for the funding provided by the Mary Gates Research Scholarship. Thanks to Rachel Spietz and Ashley Maloney for statistical analysis assistance. Finally, a huge thanks to my advisor Danny Grünbaum for all your help throughout this rigorous project.

Appendix I – Zooplankton abundance

Table 1. Abundance of organisms in each sample standardized to 1m^3 of total volume sampled.

station	sample	euph.	hyp.	gam.	*Oithona*	sm cope.	lrg cope.	larv.	chaeto.	ostra.	T Abundance	T cope.
C05	C05_25	1	1	0	233	414	10	24	33	0	714	656
	C05_50	1	53	1	236	321	101	0	0	0	712	657
	C05_75	112	154	11	464	359	330	0	0	0	1430	1153
	C05_100	35	66	0	1182	717	1573	0	0	0	3572	3471
C08	C08_25	0	0	0	709	497	175	4	24	16	1426	1381
	C08_50	0	1	2	603	232	126	8	12	29	1013	962
	C08_75	0	0	1	0	41	98	0	0	41	181	139
	C08_100	0	0	0	546	155	240	12	0	65	1019	941
C09	C09_25	0	2	1	240	143	90	0	0	49	524	473
	C09_50	0	0	0	228	269	114	4	33	12	660	611
	C09_75	0	3	2	0	20	12	0	0	65	103	33
	C09_100	0	0	0	644	118	81	12	0	90	945	843
C10	C10_25	0	3	0	306	905	8	4	57	4	1287	1218
	C10_50	2	10	2	497	285	57	0	0	37	890	839
	C10_75	19	18	2	12	94	81	0	0	98	324	187
	C10_100	1	1	0	151	126	37	0	0	94	409	314
C11	C11_25	0	0	0	485	957	0	8	41	8	1499	1442
	C11_50	0	0	0	1263	261	0	8	16	16	1565	1524
	C11_75	0	0	0	579	493	20	0	4	29	1125	1092
	C11_100	0	0	0	37	98	49	0	0	69	253	183

Table 2. Percent total abundance of zooplankton groups in each sample standardized to 1m^3 of total volume sampled. The last three columns show the percent total abundance of copepods.

station	sample	euph.	hyp.	gam.	*Oithona*	sm cope.	lrg cope.	larv.	chaeto.	ostra.	total cope.	*Oithona*	sm cope.	lrg cope.
C05	C05_25	0.1	0.1	0.0	32.6	57.9	1.3	3.3	4.7	0.0	91.8	35.5	63.0	1.4
	C05_50	0.1	7.4	0.1	33.2	45.0	14.1	0.0	0.0	0.0	92.4	36.0	48.8	15.3
	C05_75	7.8	10.8	0.8	32.5	25.1	23.1	0.0	0.0	0.0	80.6	40.3	31.1	28.6
	C05_100	1.0	1.8	0.0	33.1	20.1	44.0	0.0	0.0	0.0	97.2	34.0	20.7	45.3
C08	C08_25	0.0	0.0	0.0	49.7	34.9	12.3	0.3	1.7	1.1	96.8	51.3	36.0	12.7
	C08_50	0.0	0.1	0.2	59.5	22.9	12.5	0.8	1.2	2.8	94.9	62.7	24.2	13.1
	C08_75	0.1	0.1	0.7	0.1	22.5	54.0	0.0	0.0	22.5	76.6	0.1	29.4	70.5
	C08_100	0.0	0.0	0.0	53.6	15.2	23.6	1.2	0.0	6.4	92.3	58.0	16.5	25.5
C09	C09_25	0.0	0.3	0.2	45.9	27.2	17.1	0.0	0.0	9.3	90.2	50.9	30.2	19.0
	C09_50	0.0	0.0	0.0	34.6	40.7	17.3	0.6	4.9	1.9	92.6	37.3	44.0	18.7
	C09_75	0.0	3.0	2.2	0.0	19.8	11.9	0.0	0.0	63.2	31.6	0.0	62.5	37.5
	C09_100	0.0	0.0	0.0	68.1	12.5	8.6	1.3	0.0	9.5	89.2	76.3	14.0	9.7
C10	C10_25	0.0	0.2	0.0	23.7	70.3	0.6	0.3	4.4	0.3	94.7	25.1	74.2	0.7
	C10_50	0.2	1.1	0.2	55.9	32.1	6.4	0.0	0.0	4.1	94.3	59.2	34.0	6.8
	C10_75	6.0	5.6	0.5	3.8	28.9	25.1	0.0	0.0	30.2	57.8	6.5	50.0	43.5
	C10_100	0.1	0.2	0.0	36.8	30.9	9.0	0.0	0.0	22.9	76.7	48.1	40.3	11.7
C11	C11_25	0.0	0.0	0.0	32.3	63.9	0.0	0.5	2.7	0.5	96.2	33.6	66.4	0.0
	C11_50	0.0	0.0	0.0	80.7	16.7	0.0	0.5	1.0	1.0	97.4	82.9	17.1	0.0
	C11_75	0.0	0.0	0.0	51.4	43.8	1.8	0.0	0.4	2.5	97.1	53.0	45.1	1.9
	C11_100	0.0	0.0	0.0	14.5	38.7	19.4	0.0	0.0	27.4	72.6	20.0	53.3	26.7

Appendix II – Environmental parameters

Table 3. Environmental parameters (mean ± SE) measured at all stations, characterizing the ecological conditions for each samples collected.

station	depth (m)	sample	mean sal	mean dO2 (mL/L)	mean pH	mean poTemp (°C)	mean fluorescence
C05	169	C05_25	31.0653 ± 0.08	5.0050 ± 0.06	8.2989 ± 0.01	10.6823 ± 0.03	2.1034 ± 0.02
		C05_50	31.6411 ± 0.02	5.1594 ± 0.03	8.4208 ± 0.01	10.6927 ± 0.01	2.3070 ± 0.02
		C05_75	32.3663 ± 0.07	2.2654 ± 0.36	8.3303 ± 0.02	9.9097 ± 0.12	2.0514 ± 0.04
		C05_100	32.8718 ± 0.01	0.1530 ± 0.01	8.0656 ± 0.01	8.7846 ± 0.02	1.8125 ± 0.00
C08	273	C08_25	30.4894 ± 0.07	5.3769 ± 0.07	8.2449 ± 0.00	10.5462 ± 0.08	2.1999 ± 0.03
		C08_50	31.5789 ± 0.04	3.9482 ± 0.08	8.2358 ± 0.00	11.3221 ± 0.04	1.9324 ± 0.01
		C08_75	32.5054 ± 0.05	1.4518 ± 0.13	8.1515 ± 0.01	9.7587 ± 0.13	1.8283 ± 0.01
		C08_100	32.8314 ± 0.01	0.8491 ± 0.01	8.0619 ± 0.00	8.7389 ± 0.02	1.7854 ± 0.00
C09	362	C09_25	30.4174 ± 0.10	5.2475 ± 0.05	8.3477 ± 0.00	10.6132 ± 0.07	2.1205 ± 0.04
		C09_50	31.5993 ± 0.05	4.0317 ± 0.09	8.3045 ± 0.00	11.9585 ± 0.06	1.8465 ± 0.01
		C09_75	32.4555 ± 0.05	1.2192 ± 0.17	8.1900 ± 0.01	9.9178 ± 0.19	1.7782 ± 0.00
		C09_100	32.8434 ± 0.01	0.7809 ± 0.02	8.0848 ± 0.00	8.6470 ± 0.02	1.7405 ± 0.00
C10	360	C10_25	30.2198 ± 0.14	5.2158 ± 0.05	8.3647 ± 0.00	10.6235 ± 0.07	2.1597 ± 0.04
		C10_50	31.5838 ± 0.07	4.0147 ± 0.11	8.3212 ± 0.00	12.0087 ± 0.08	1.8771 ± 0.01
		C10_75	32.4333 ± 0.04	1.0612 ± 0.20	8.2018 ± 0.01	10.0068 ± 0.21	1.7970 ± 0.00
		C10_100	32.8175 ± 0.01	0.4957 ± 0.01	8.0842 ± 0.00	8.5473 ± 0.02	1.7684 ± 0.00
C11	159	C11_25	29.8932 ± 0.38	5.0532 ± 0.07	8.3679 ± 0.01	10.9396 ± 0.13	2.2648 ± 0.08
		C11_50	31.6612 ± 0.06	3.9010 ± 0.08	8.3172 ± 0.00	12.6080 ± 0.08	1.9213 ± 0.02
		C11_75	32.4053 ± 0.04	1.0544 ± 0.22	8.2131 ± 0.01	10.1490 ± 0.23	1.8257 ± 0.00
		C11_100	32.7665 ± 0.01	0.1215 ± 0.01	8.0838 ± 0.01	8.4679 ± 0.02	1.8006 ± 0.00

Appendix III – PCA including all samples

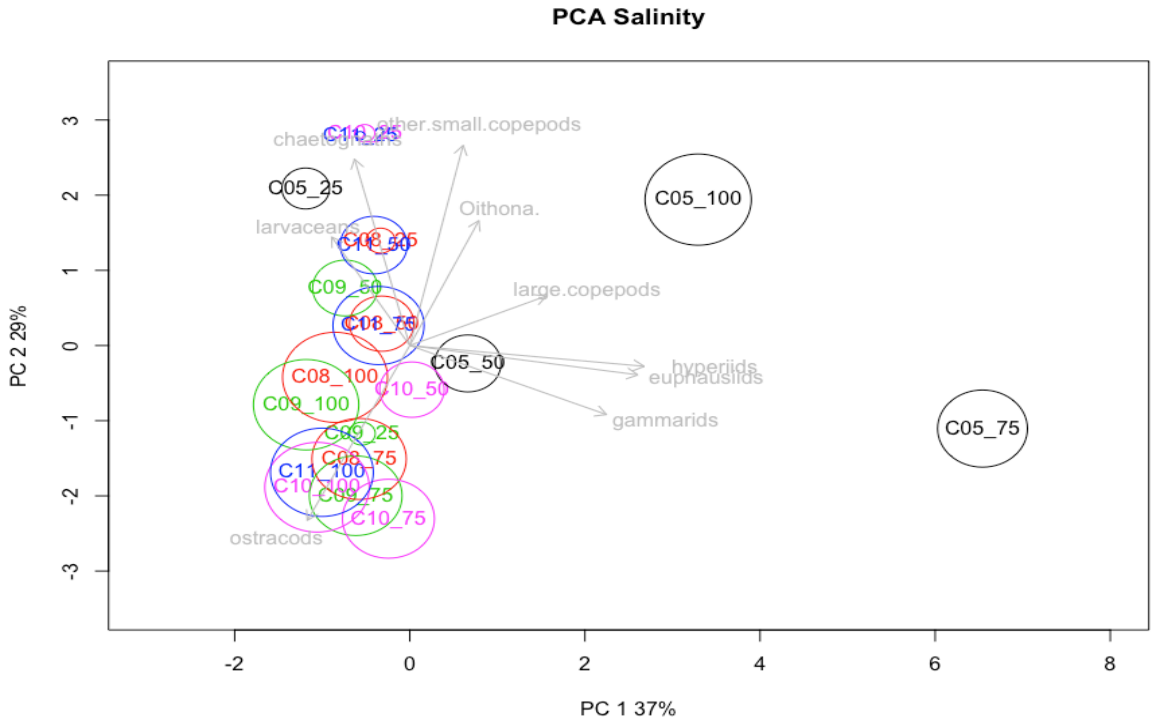

Fig. 1. Principal component analysis of species composition for each sample, with circles scaled to mean salinity values of depth ranges sampled. The vectors show the correlation of taxa with principal component 1 and principal component 2.

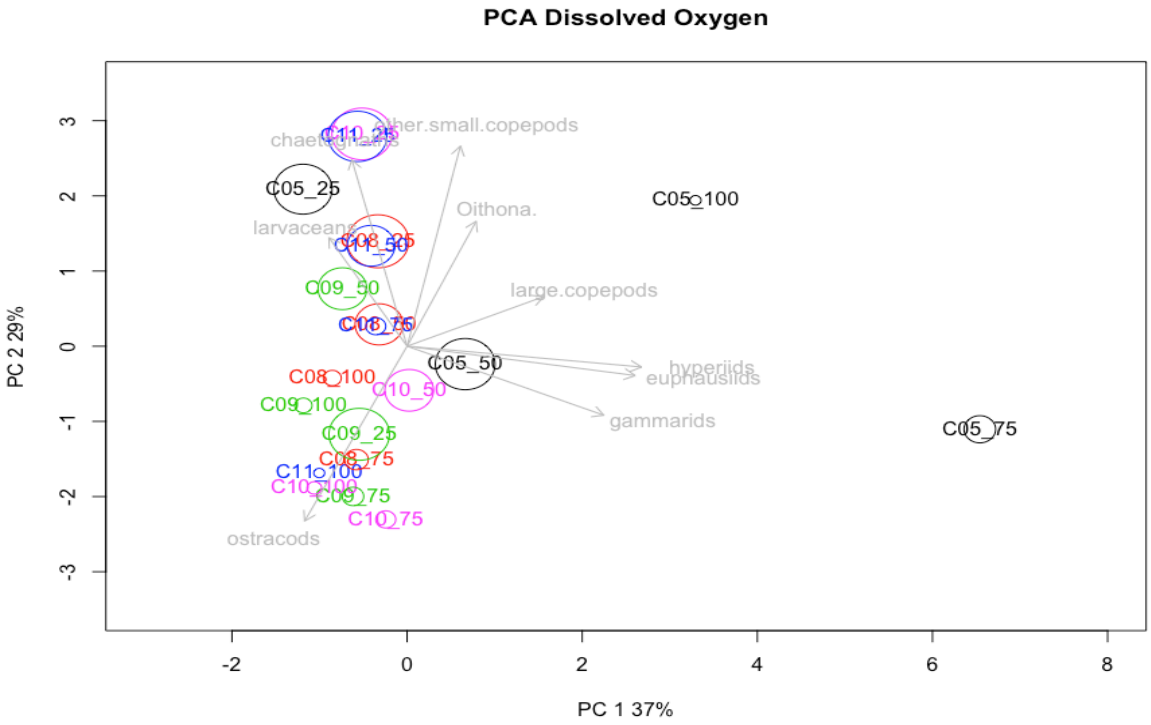

Fig. 2. Principal component analysis of species composition for each sample, with circles scaled to mean dissolved oxygen values of depth ranges sampled. The vectors show the correlation of taxa with principal component 1 and principal component 2.

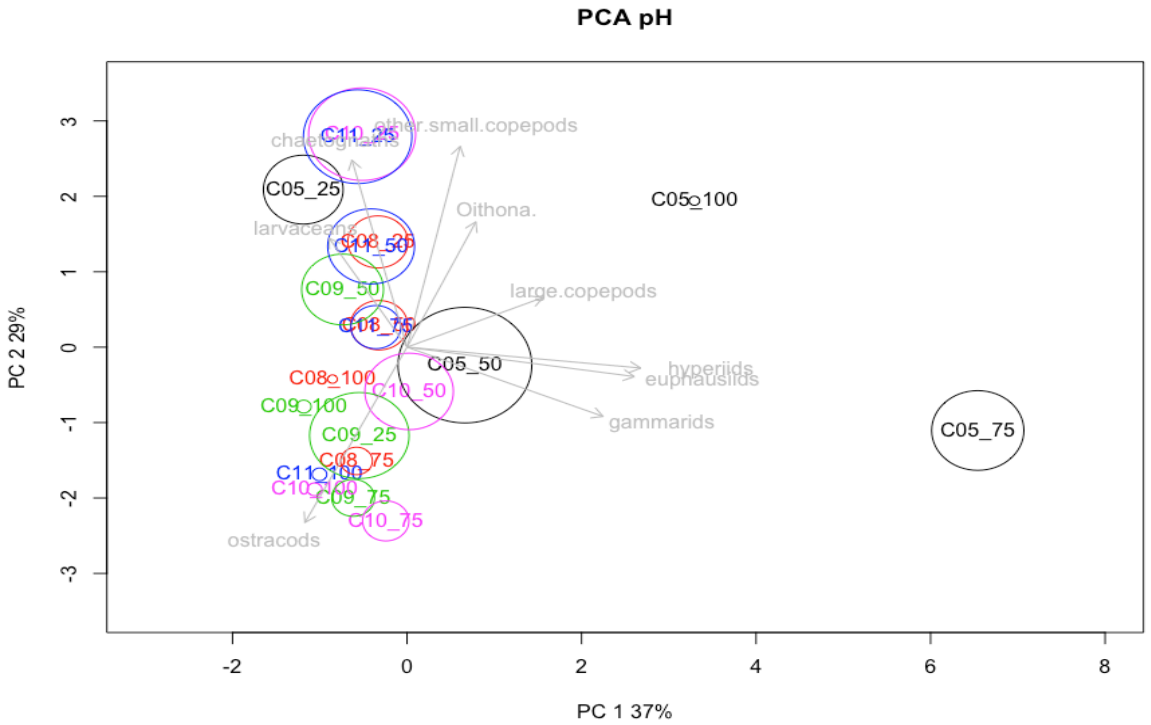

Fig. 3. Principal component analysis of species composition for each sample, with circles scaled to mean pH values of depth ranges sampled. The vectors show the correlation of taxa with principal component 1 and principal component 2.

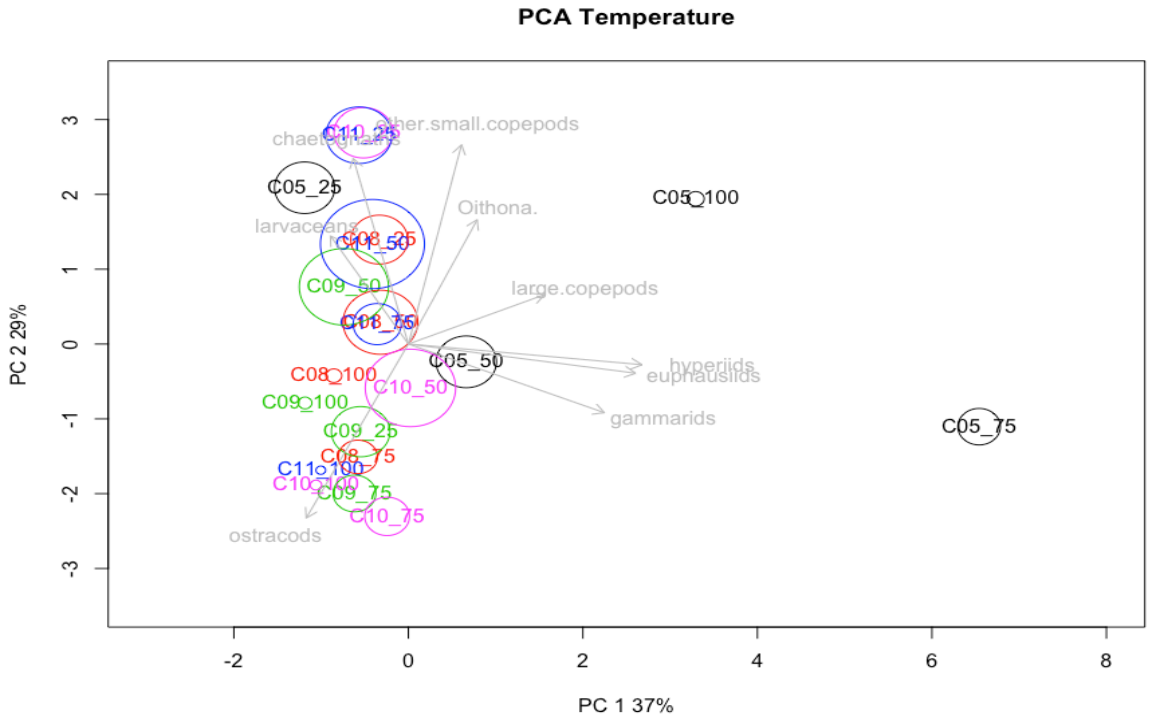

Fig. 4. Principal component analysis of species composition for each sample, with circles scaled to mean potential temperature values of depth ranges sampled. The vectors show the correlation of taxa with principal component 1 and principal component 2.

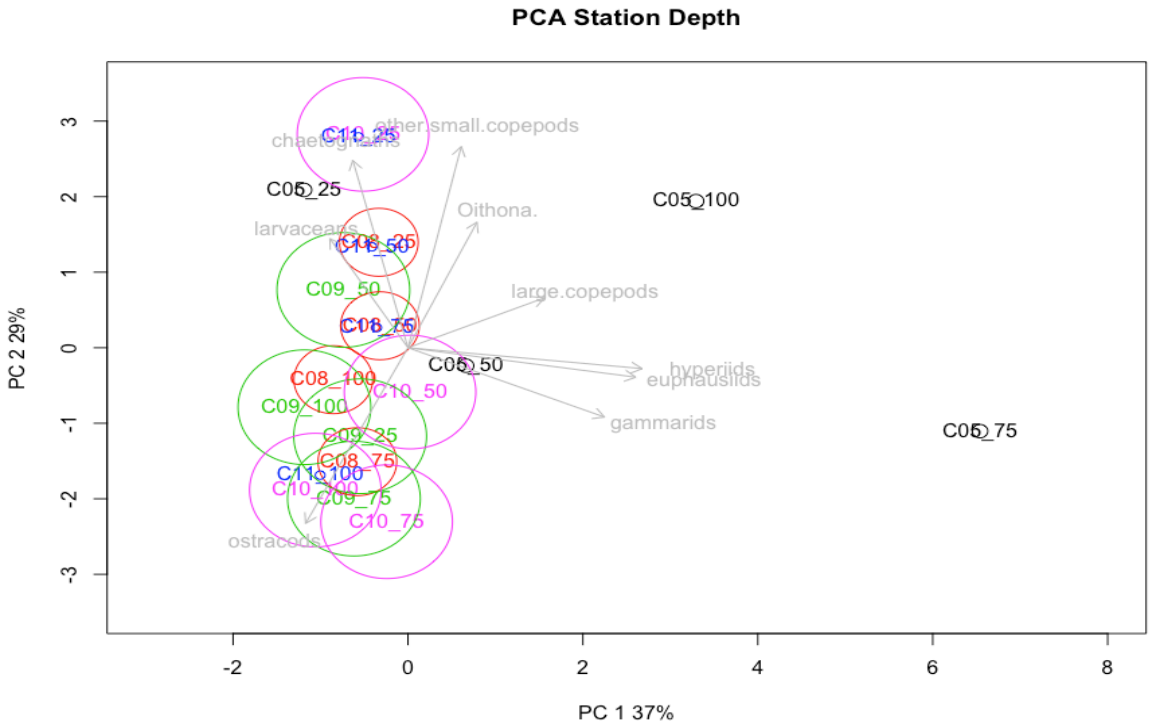

Fig. 5. Principal component analysis of species composition for each sample, with circles scaled to station depth. The vectors show the correlation of taxa with principal component 1 and principal component 2.

Appendix IV – PCA of Muchalat samples

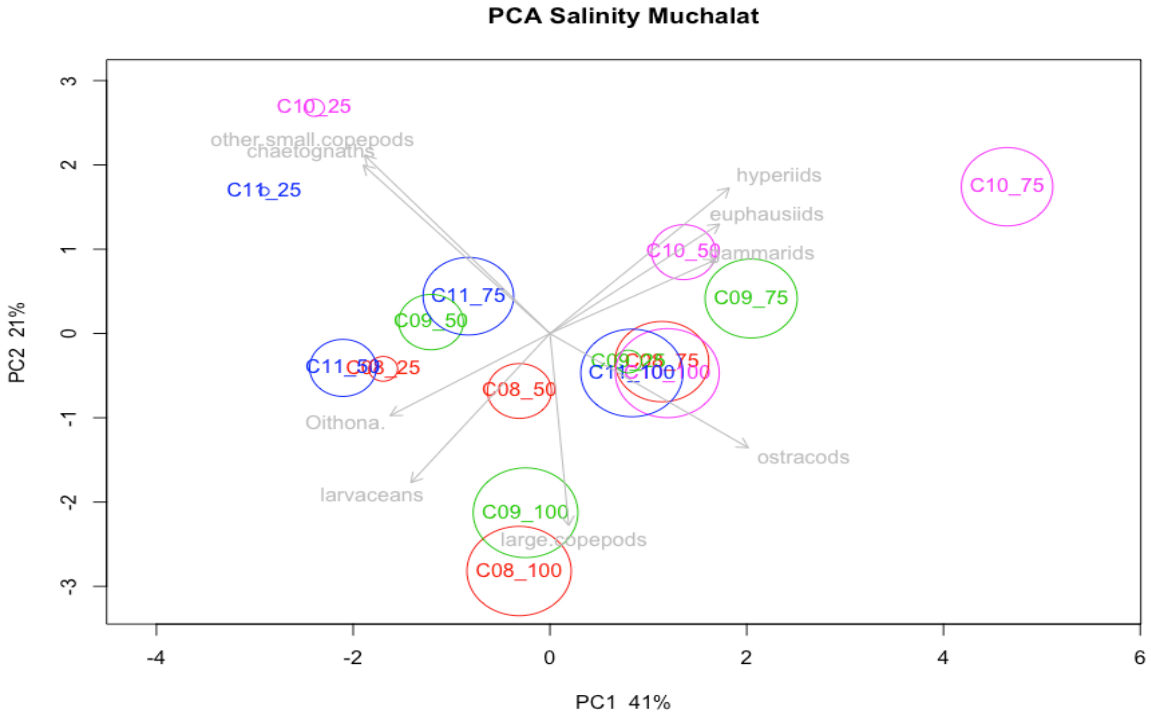

Fig. 6. Principal component analysis of species composition for Muchalat Inlet samples, with circles scaled mean salinity values of depth ranges sampled. The vectors show the correlation of taxa with principal component 1 and principal component 2.

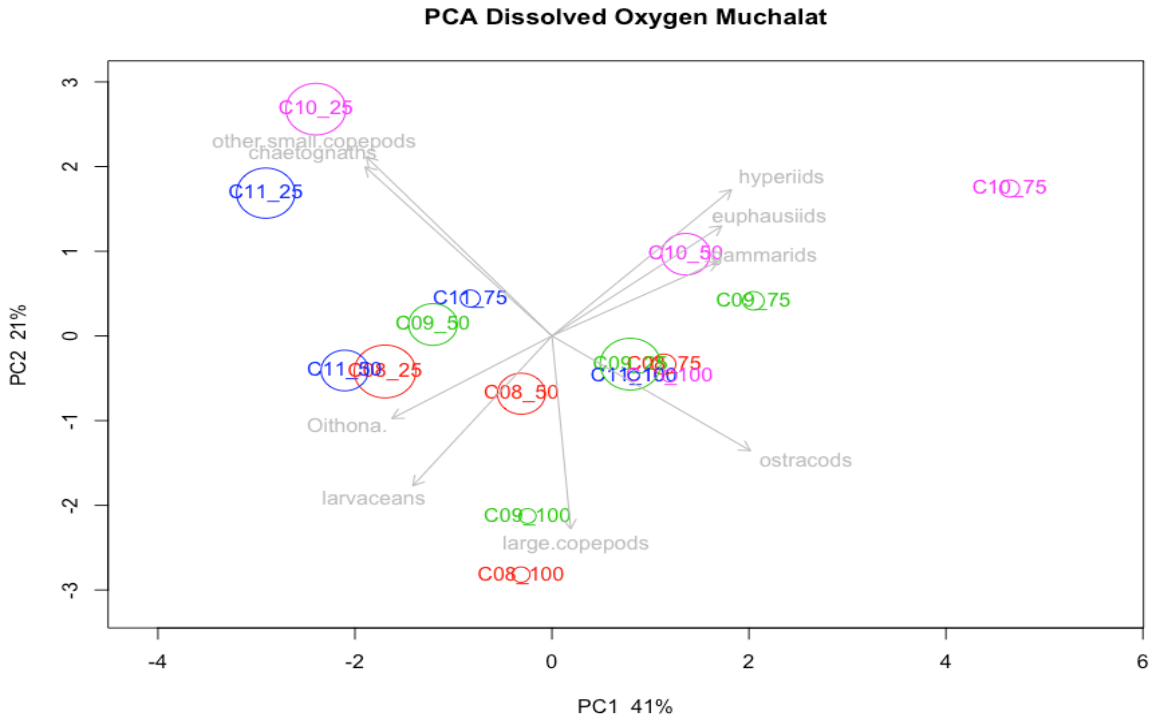

Fig. 7. Principal component analysis of species composition for Muchalat Inlet samples, with circles scaled mean dissolved oxygen values of depth ranges sampled. The vectors show the correlation of taxa with principal component 1 and principal component 2.

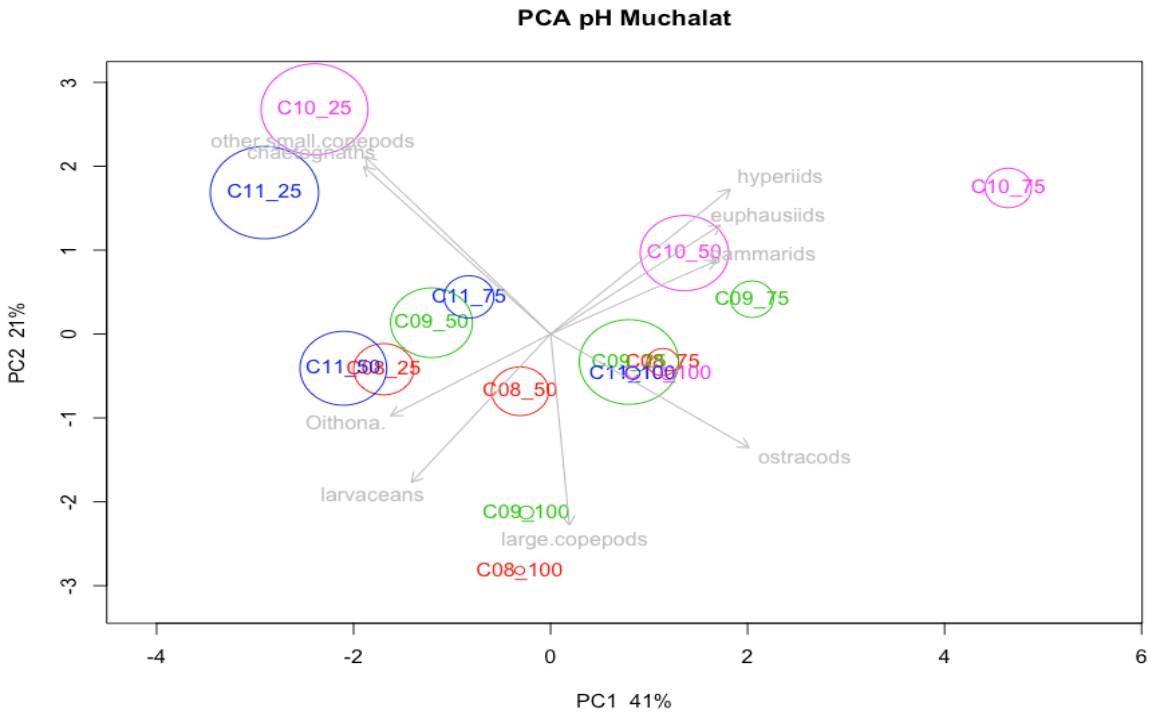

Fig. 8. Principal component analysis of species composition for Muchalat Inlet samples, with circles scaled mean pH values of depth ranges sampled. The vectors show the correlation of taxa with principal component 1 and principal component 2.

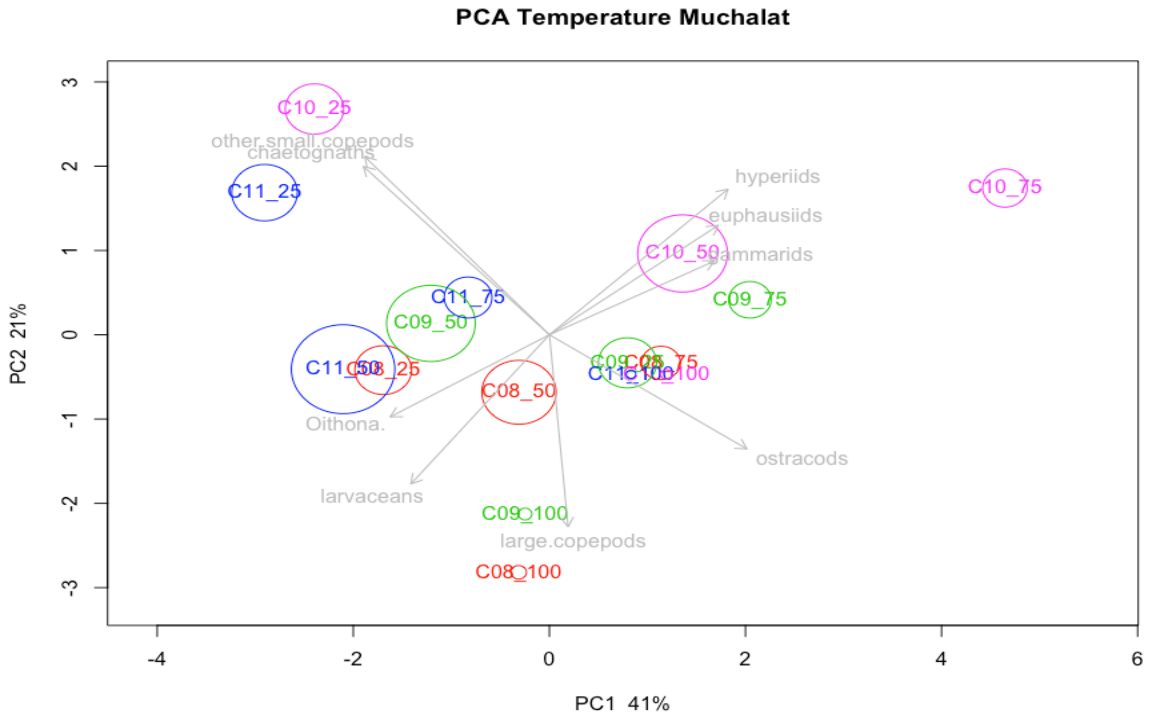

Fig. 9. Principal component analysis of species composition for Muchalat Inlet samples, with circles scaled mean potential temperature values of depth ranges sampled. The vectors show the correlation of taxa with principal component 1 and principal component 2.

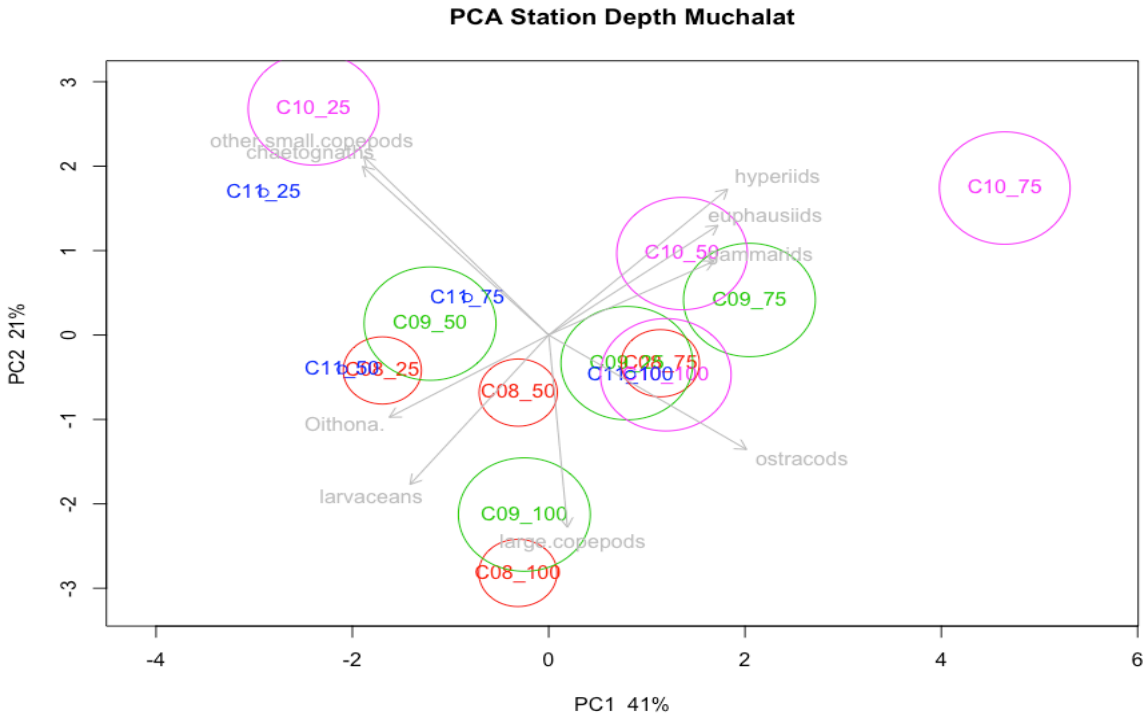

Fig. 10. Principal component analysis of species composition for Muchalat Inlet samples, with circles scaled to station depth. The vectors show the correlation of taxa with principal component 1 and principal component 2.

Appendix V – Shannon Wiener Diversity Index

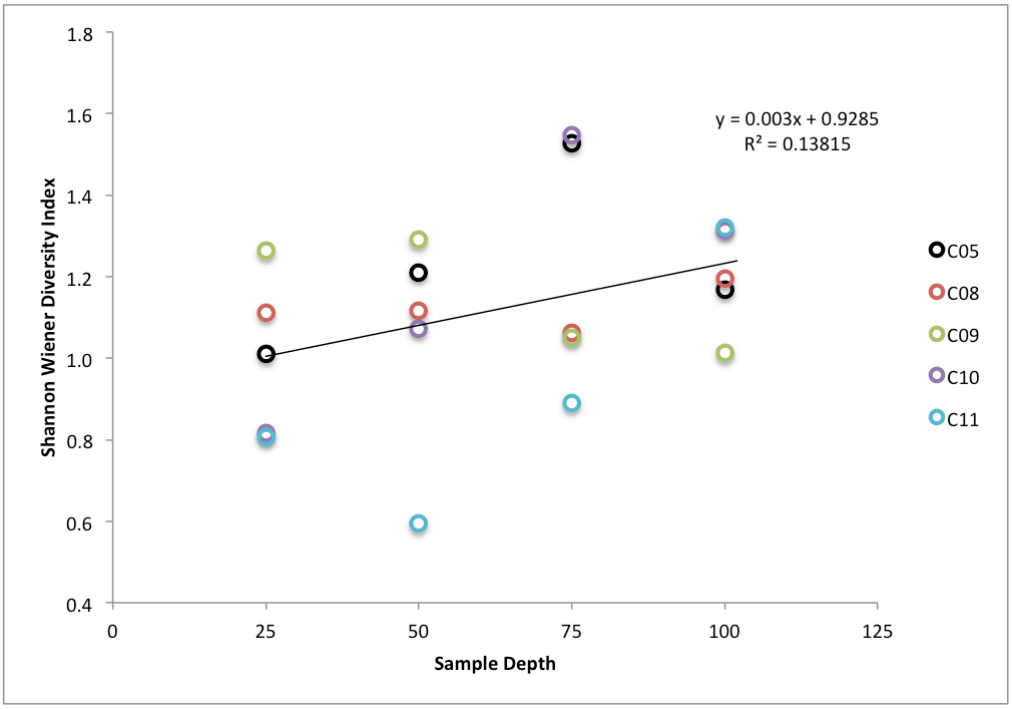

Fig. 11. Shannon Wiener Diversity Index values reported for each sample. Colors categorize values by station.

Appendix VI – Underwater Video Profiler application

The alternative applies a technological approach to this investigation on zooplankton populations through development and implementation of and Underwater Video Profiler (UVP), designed to capture and store imaging data of zooplankton against tidal flow. The instrument was deployed in Puget Sound at night, just north of Shilshole Marina offshore from Golden Gardens Beach Park. This approach allows for a much greater sample size and improved spatial resolution of overall zooplankton abundance, but comes at the cost of lower taxonomic resolution, providing less insight on zooplankton community composition. Here we compare the difference in imaging data between onshore and offshore stations, and associated environmental conditions. Here it should be stated that UVP sampling and video data analysis remains largely incomplete. The primary objective here was to successfully design, build and deploy an underwater video profiler prototype as to explore this zooplankton sampling technique for future applications.

UVP sensor design

An underwater video profiler (UVP) was constructed in the Oceanography Technology Center at the University of Washington, in collaboration with Daniel Grünbaum. The technical components of the imager included HD 1080P USB CMOS board camera module, ODROID-C1+ computer, microSD card, Ethernet, Sensus depth probe, external flashlights, and battery power.

The waterproof housing was constructed out of industrial PVC plumbing materials and PVC cement. Two 1’ long, 3” diameter PVC pipes, connected in the middle by a 3” slip socket, encompassed the battery unit (back) and the imager

(front). A circular 3" diameter faceplate was cut from 3/8" polycarbonate (LEXAN) sheet and sealed by a 3" slip socket and O-ring. A grooved cap plate enclosed the back end of the housing, sealed with PVC cement.

External flashlights (2) were constructed in a similar fashion, with 2' long, 2" diameter PVC piping. The housing was filled with 8 D-cell batteries in the back end, wired to a 2.1 Watt LED light in the front. The back of the housing was capped and sealed with PVC cement. The front included a 2" slip socket and O-ring sealed to a transparent polycarbonate (LEXAN) faceplate. A switch was installed to manually turn the lights on and off. Styrofoam was used to position the light and switch near the faceplate.

The entire unit was fitted to an aluminum plate by U-bolts, and the towline attached to the top of the frame. The flashlights were fitted to the plate, and positioned to maximize illumination within the camera's field of view. A 15kg lead weight was attached to the bottom of the unit to ensure negative buoyancy and maximize stabilization.

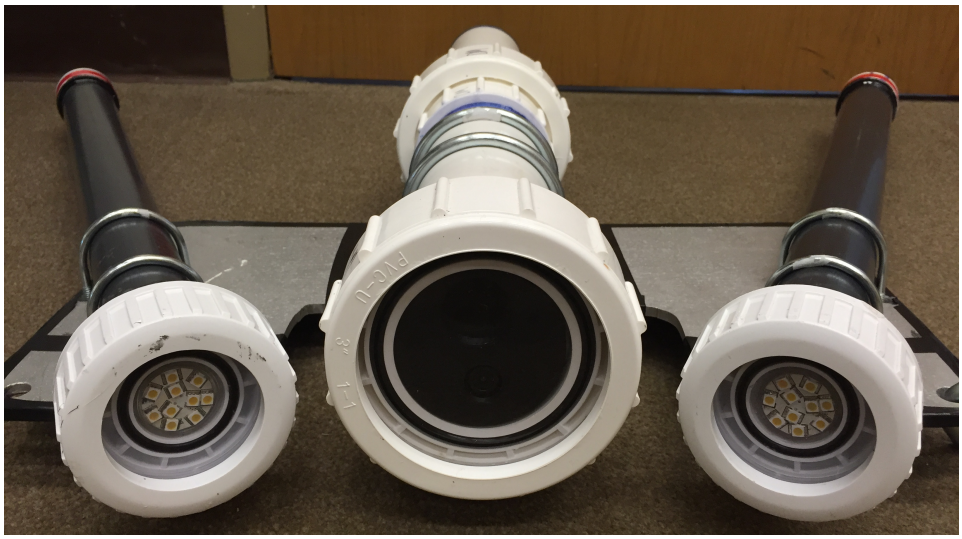

UVP sampling methods

The UVP was deployed offshore from Shilshole Marina aboard the R/V *Barnes* at night. Six stations were selected for sampling, three stations near shore and three stations perpendicular offshore, approximately equidistant apart. CTD casts were conducted at each station to measure vertical profiles of salinity, dissolved oxygen, fluorescence, and pH parameters for the upper 30m of the water column. The UVP was deployed to 15m depths at each station and the vessel drifted for 5 minutes while imaging data was recorded against the current. The UVP was programmed to capture images on 2-minute intervals to produce replicates for each station sampled.

Image 2. Station and transect map of UVP stations north of Shilshole Marina perpendicular to shore off Golden Gardens Beach Park. Stations are numbered in order sampled.

UVP data analysis

The imager data was quantified using video analysis software to optimize particles captured. Digital image filters were applied to detect motion of pixels across multiple frames and gray-scaled to optimize images of particles captured.

Particles were categorized by size, small, medium and large, and we assume that all particles represent zooplankton, determined by the limits implemented by size filters applied.

UVP Results

Here it should be stated that the UVP sampling and video data analysis remains largely incomplete. The primary objective here was to successfully design, build and deploy an underwater video profiler prototype as to explore this zooplankton sampling technique for future applications.

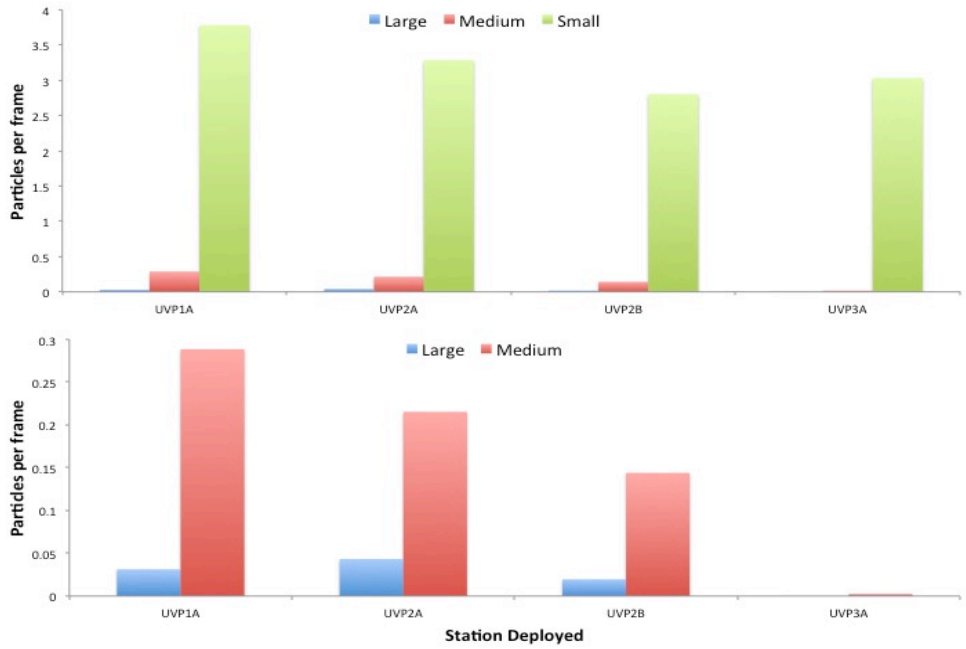

Fig. 12. Raw video data is presented as abundance of particles per frame. Particles were classified by number of pixels, where small represents 50-500 pixels, medium represents 500-5,000 pixels, and large represents 5,000=50,000 pixels.

REFERENCES

Clutter, R. J., and M. Anraku. 1979. Zooplankton sampling. 3. impr. Unesco, Paris.

Frederiksen, M., M. Edwards, A. J. Richardson, N. C. Halliday, and S. Wanless. 2006. From plankton to top predators: bottom-up control of a marine food web across four trophic levels. Journal of Animal Ecology 75:1259–1268.

Gentleman, W., A. Leising, B. Frost, S. Strom, and J. Murray. 2003. Functional responses for zooplankton feeding on multiple resources: a review of assumptions and biological dynamics. Deep Sea Research Part II: Topical Studies in Oceanography 50:2847–2875.

Gold River Discharge. 1956. . Historical Data, Government of Canada Wateroffice, Gold River.

Gorsky, G., P. R. Flood, M. Youngbluth, M. Picheral, and J.-M. Grisoni. 2000a. Zooplankton Distribution in Four Western Norwegian Fjords. Estuarine, Coastal and Shelf Science 50:129–135.

Gorsky, G., M. Picheral, and L. Stemmann. 2000b. Use of the Underwater Video Profiler for the Study of Aggregate Dynamics in the North Mediterranean. Estuarine, Coastal and Shelf Science 50:121–128.

Hays, G. C. 2003. A review of the adaptive significance and ecosystem consequences of zooplankton diel vertical migrations. Hydrobiologia 503:163–170.

Laprise, R., and J. J. Dodson. 1994. Environmental variability as a factor controlling spatial patterns in distribution and species diversity of zooplankton in the St. Lawrence Estuary. Marine Ecology-Progress Series 107:67–67.

Longhurst, A. R. 1991. Role of the marine biosphere in the global carbon cycle. Limnology and Oceanography 36:1507–1526.

Pelle, B. C. 2015. Analysis of zooplankton species composition and depth-based habitat preference in Nootka Sound, B.C., Canada.

Pickard, G. L. 1963. Oceanographic Characteristics of Inlets of Vancouver Island, British Columbia. Journal of the Fisheries Research Board of Canada 20:1109–1144.

Shaffer, G. 1993. Effects of the Marine Biota on Global Carbon Cycling. Pages 431–455 *in* M. Heimann, editor. The Global Carbon Cycle. Springer Berlin Heidelberg.

Silva, N., and C. A. Vargas. 2014. Hypoxia in Chilean Patagonian Fjords. Progress in Oceanography 129:62–74.

Stalder, L. C., and N. H. Marcus. 1997. Zooplankton responses to hypoxia: behavioral patterns and survival of three species of calanoid copepods. Marine Biology 127:599–607.

Turner, J. T. 2002. Zooplankton fecal pellets, marine snow and sinking phytoplankton blooms. Aquatic Microbial Ecology 27:57–102.

Turner, J. T. 2004. The Importance of Small Planktonic Copepods and Their Roles in Pelagic Marine Food Webs. Zoological Studies 43.

Tyson, R. V., and T. H. Pearson. 1991. Modern and ancient continental shelf anoxia: an overview. Geological Society, London, Special Publications 58:1–24.